VIA MEDICA

Nuclear Medicine Review 2001
Vol. 4, No. 1, pp. 27–33

ISSN 1506–9680

Original

Comparison of functional imaging and standard CT in evaluation of disease extent in patients with tumours showing neuroendocrine features

Jarosław B. Ćwikła[1], John R. Buscombe[1], Waldemar A. Mielcarek[2], Martyn E. Caplin[3], Anthony J. Watkinson[4], Andrew J.W. Hilson[1]

[1]Department of Nuclear Medicine, Royal Free Hospital, London, UK
[2]Department of Nuclear Medicine, Central Military Academy, CSK WAM, Warszawa, Poland
[3]Neuroendocrine Tumour Clinic (NET), Royal Free Hospital, London, UK
[4]Department of Radiology, Royal Free Hospital, London, UK

Abstract

BACKGROUND: The diagnostic approach that should be used in disseminated neuroendocrine tumours (NET) remains a significant clinical problem. A novel approach has been the use of ^{111}In Octreotide as functional imaging to find NETs. Therefore, the aim of this retrospective study is to report our comparison with direct CT as standard anatomical imaging.

MATERIAL AND METHODS: A total of 48 patients (aged 16–79 years; mean age 55, SD 14 years) were imaged using both techniques with final histological confirmation of NET. Histology was as follows: 26 carcinoids; 2 pheochromocytomas; 4 gastrinomas, 1 islet tumour; 2 paragangliomas, 1 modullary carcinoma of the thyroid, 8 undetermined NET and 4 other tumours with signs of neuro-ectodermal cancers (2 hepatocellular carcinomas (HCC), fibrolamellar HCC and fibrous tumour). All patients had ^{111}In Octreotide and 30 had ^{123}I mIBG scans followed by spiral CT with contrast enhancement. 26 patients had single functional scans and 22 had multiple, up to 6 scans. Extent of disease as number of lesions was compared between CT and octreotide.

RESULTS: CT was the best modality in 11 patients, in 6 it was as good as ^{111}In Octreotide. mIBG was the best in 6 patients; in 3 patients mIBG was as good as octreotide study. In 22 patients ^{111}In Octreotide was the most effective modality. In one patient there was no advantage with any of the tests. Comparison of the number of organs involved indicated that an octreotide study was much more effective than CT scanning (Wilcoxon matched pairs test, $p < 0.001$) and also the overall number of lesions detected using ^{111}In Octreotide was greater than with CT (Wilcoxon Matched Pairs test $p < 0.01$).

CONCLUSION: Our results confirm the recommendation of the European NET group that functional imaging should be performed in patients with suspected NET.

Key words: ^{123}I mIBG, ^{111}In Octreotide, CT, neuroendocrine, tumours

Correspondence to: Jarosław B. Ćwikła, MD
Department of Nuclear Medicine
Royal Free Hospital, London NW3 2QG
Tel: (+44) 207 830 2470, fax: (+44) 207 830 2469
e-mail: buscombe@rfhsm.ac.uk

Introduction

Neuroendocrine tumours are today considered tumours derived from the diffuse neuroendocrine system, which is made up of peptide- and amine-producing cells with different hormonal profiles depending on their site of origin [1]. Carcinoid tumours are classified as neuroendocrine tumours and share cytochemical features with melanomas, pheochromocytomas, medullary carcinoma of the thyroid and pancreatic endocrine tumours [1–3]. Each type is histologically similar to each other and to carcinoid tumours [4, 5].

Except for insulinoma, each is malignant in most (more than 60%) if not all cases [4]. They are also a vascular tumour with similar radiographic appearance and metastatic pattern (primarily to regional lymph nodes and to liver). Octreotide, a semi-synthetic, somatostatin analogue, has a significant role to play in the

palliation of the symptoms when there is extensive tumour. It appears to have a good affinity for the SS2 and SS3 receptors available in most neuroendocrine tumours [6–8]. It is not generally thought to be tumoricidal but can help to reduce the production of hormone (for example 5-hydroxytryptamine from carcinoid and gastrin from gastrinoma).

NETs can also express amine receptors and as a result have been found to accumulate ^{123}I iodine metaiodobenzylguanidine (mIBG). This was the first radiopharmaceutical used to image these tumours, although it is now known that this procedure is less sensitive than ^{111}In Octreotide imaging [9, 10]. mIBG is particularly effective in pheochromocytomas which are derived from the sympathetic nervous system and related structures [11, 12]. However, uptake of the ^{123}I, (^{131}I) mIBG in NETs is often poor [8, 12].

A variety of anatomical imaging techniques has been used to locate NET, each of which exhibits important drawbacks. For instance, since approximately 90% of pheochromocytomas occur within the adrenal glands, computed tomography (CT) of the adrenal glands has been found efficacious [13]. However, CT depicts only anatomic abnormalities and, while this approach is the most popular in clinical practice, it seems to be less accurate than functional approaches in the detection of primary, recurrent and metastatic NETs.

^{111}In Octreotide is now considered to be the most sensitive imaging modality for metastatic neuroendocrine tumours. The greater sensitivity of ^{111}In Octreotide in imaging NETs is achieved by the presence of specific receptors and the internalising of the radiotracer by the NET cells [14].

The aim of this retrospective study is to report our comparison of the functional approach with direct CT as standard anatomical imaging.

Material and methods

Overall 48 patients with suspected NET were retrospectively evaluated. Mean age of patients was 55 years old (range 16–79; SD 14). All patients came from the NET clinic and were assessed in standard clinical proceedings. As all studies were performed for clinical reasons and this was a retrospective review of the collected data, ethical committee approval was not required.

^{111}In Octreotide imaging

A mean of 180–200 MBq of ^{111}In Octreotide Mallinckodt, (Nuclear Medicine Petten Netherlands) i.v. injection was performed in each case. Whole body planar images and SPECT were acquired up to 24 hours. Planar images were obtained using both heads with speed 10 cm/min, raw and truncated anterior and posterior data were displayed and printed as a hard copy in each case.

All imaging was performed using a double head SPECT gamma camera Picker Prism 2000 XP (Picker International, Cleveland, OH, USA) interfaced to the computer workstation Odyssey VP (Picker Int., Cleveland, OH, USA). Images were acquired in 64 $\times$ 64 matrix. All patients were imaged with medium-energy collimators for 170 KeV, and 240 KeV 20% energy windows (Picker Int., Cleveland, OH, USA). The tomographic data were acquired in 30 steps, over 180 degree for each head of the gamma camera. The minimum separation between the patient and the collimators was obtained using elliptical orbit. Data acquisition time was 30 s per one step. Tomographic reconstruction was performed using a Ramp back-projection filter or Iterative reconstruction. These images were then smoothed using an automatically applied count optimised post-projection 3D Metz filter or manual Butterworth filter with order of 7.0–11.0 and cut-off at 0.2–0.3. Attenuation correction and scatter correction were not performed. At this stage the data was prepared for re-orientation into orthogonal slices. Slice thickness was 9.4 mm for medium-energy collimation in each case. Images were displayed as re-orientated transverse, coronal and sagittal slices. Hard copy of images was acquired using the Helios system (Polaroid, USA).

^{123}I mIBG imaging

^{123}I mIBG was prepared in the Department of Nuclear Medicine at the Royal Free Hospital (purchased from Amersham, (UK). Mean 130–160 MBq of ^{123}I mIBG i.v. injection was performed in 36 subjects. Whole body scan and 24 h SPECT were performed. Tomographic imaging was performed using a double head SPECT gamma camera Picker Prism 2000 XP (Picker Int., Cleveland, OH, USA) interfaced to the computer workstation Odyssey VP (Picker Int., Cleveland, OH, USA). Whole body planar images were acquired using both heads with speed 10cm/min, raw and truncated anterior and posterior data were displayed and printed as a hard copy. Tomographic images were acquired in a 128 $\times$ 128 matrix. All patients were imaged with low-energy collimators with 20% energy windows for ^{123}I (Picker Int., Cleveland, OH, USA). The tomographic data were acquired in 30 steps, over 180 degree for each head of the gamma camera. The minimum separation between the patient and the collimators was made using elliptical orbit. Data acquisition time was 30 s per one step. As previously described, tomographic reconstruction was performed using a Ramp back-projection filter or iterative reconstruction. These images were then smoothed using an automatically applied count optimised post-projection 3D Metz filter or manual Butterworth filter with order of 7.0–11.0 and cut-off at 0.2–0.3. Attenuation correction and scatter correction were not performed. At this stage the data was prepared for re-orientation into orthogonal slices. Slice thickness was 7.5 mm for low-energy collimation. Images were displayed as re-orientated transverse, coronal and sagittal slices. Hard copy of images was acquired using the Helios system (Polaroid, USA).

CT imaging

In most patients triple phase scan of the liver with post-contrast scans of the chest and pelvis using standard spiral CT (HiSpeed Adv. System Philips, Netherlands) was performed. An intravenous bolus of approximately 150 ml non-ionic (Omnipaque 300; Nycomed-Amersham, Princeton, NJ, USA) contrast material was administered at a rate of 2 ml/sec followed by acquisition of 7 mm- to 10 mm-thick contiguous axial sections through the thorax, abdomen or pelvis, depending on the site of the principal tumour.

Image analysis

Scintigraphy images were reviewed by nuclear imaging physicians. CT images were read by trained radiologists. The images for each patient were presented in random order, scintigraphy using both ^{111}In Octreotide and ^{123}I mIBG was followed by CT. Results of other studies (imaging and biochemistry) were not revealed prior to analysis of the CT and scintigraphy images. All scintigraphy im-

ages were evaluated using quality image interpretation. Organs that normally accumulate the tracers were identified by means of visual score. Sites of accumulation that did not conform to the usual anatomic configurations of normal sites of radiotracer accumulation were considered as abnormal.

Parts of the body were evaluated using simple method, which categorised the organs as follows: liver, adrenals, pancreas, lungs, mediastinum, periaortic nodes, abdominal lesions including bowel, omental or peritoneal lesions, pelvis, pancreas, spleen, chest, spine, skull, neck and extremities, all were evaluated based on tomographic imaging. In each case, pathological lesions detected in visual inspection were counted for each diagnostic modality separately. All detected lesions were superimposed into organs or part of the body. All lesions were counted using simple calculation as 1) a single lesion, 2) a few (less then 5) and 3) more than 5 lesions, using simple score as 1, 2 and 3 respectively. Then all were recounted in the same way for each modality separately. Additional organs and parts of the body involved were counted to assess tumour extent without calculation of single lesions. Finally separate liver metastatic lesions were counted using simple score as mentioned above.

Statistical analysis

Comparison of both anatomical and functional approach in evaluation of number of lesions, number of separate organs or parts of the body involved and a number of liver deposits were performed using non-parametric Wilcoxon Matched Pairs test; ($p < 0.05$ as significant) due to non-linear distribution. Comparison of differences between each modality within the selected group of patients with different kinds of tumour was performed using the non-parametric Mann-Whitney U test ($p < 0.05$ as significant, Statistica 4.5, Statsoft, OK, USA).

Results

All patients had ^{111}In Octreotide and 30 had ^{123}I mIBG scans followed by standard CT with contrast enhancement. All patients had histological confirmation of pathology. Recurrent disease was noted in 11 subjects. Mean age of all patients was 55 years (range 16–79 years, SD 14). Histology confirmed presence in 26 patients of carcinoid tumours, in 2 patients of pheochromocytoma, in 4 subjects of gastrinoma, and in one patient of islet tumour, in 2 patients of paraganglioma and in one patient of medullary thyroid carcinoma (MCT). There were also 8 undetermined NETs and finally 4 patients presented other tumours with signs of neuro-ectodermal neoplasm (2 hepatocellular carcinoma — HCC; single fibrolamellar HCC and single fibrous HCC tumour). Clinical details are presented in Table 1 for patients with carcinoid tumours, in Table 2 for patients with other differentiated NET tumours (gastrinoma, islet cell, MCT; pheochromocytoma, paraganglioma), and in Table 3 for undetermined NET or those with NET signs.

Stage of disease, as number of the lesions and extent of disease, was compared between CT and octreotide study. CT was the best modality in 11 patients; in 6 it was as good as ^{111}In octreotide (e.g. Fig. 1), e. ^{123}I mIBG study was the best in 6 patients; in 3 patients mIBG was as good as octreotide study (e.g. Fig. 2).

Table 1. Clinical details of all patients with presented carcinoid tumours

Patient	Age	Histology	Localisation	Clinical details
1	16	Carcinoid	Appendix	Carcinoid of appendix 13 mm of size
2	64	Carcinoid	Abdomen	Abdominal carcinoid
3	57	Carcinoid	Gastro/oesophagal	Recurrent gastro-oesophagal 1993
4	54	Carcinoid	Right bronchus	Pulmonary carcinoid
5	70	Carcinoid	Caecum	Carcinoid of the caecum
6	56	Carcinoid	Testis	Recurrent carcinoid — 1993
7	61	Carcinoid	Ileum	Ileum carcinoid
8	52	Carcinoid	Neck lymph node	Recurrent neck carcinoid
9	70	Carcinoid	Ovary carcinoid	Ovary carcinoid
10	45	Carcinoid	Appendix	Carcinoid of appendix
11	55	Carcinoid	Ampulla	Recurrent ampullary carcinoid
12	56	Carcinoid	Caecum, ileum	Caecal and terminal ileum carcinoid
13	72	Carcinoid	Liver	Disseminated carcinoid
14	79	Carcinoid	Ileum	Small ileal tumour
15	43	Carcinoid	Pancreas	Carcinoid/MEN1
16	66	Carcinoid	Liver	Disseminated carcinoid
17	61	Carcinoid	Pancreas head	Head of pancreas and liver metastasis
18	44	Carcinoid	Liver	Multiple liver tumour
19	40	Carcinoid	Ampulla	Carcinoid tumour of duodenum
20	30	Carcinoid	Colon	Recurrent carcinoid liver metastasis
21	31	Carcinoid	Colon	Large bowel carcinoid
22	70	Carcinoid	Pancreas	Abdominal nodes
23	73	Carcinoid	Small bowel	Disseminated carcinoid
24	52	Carcinoid	No origin	Disseminated carcinoid
25	74	Carcinoid	Stomach	Recurrent carcinoid liver metastasis
26	58	Carcinoid	Caecum, ileum	Appendix lymph node metastasis

Table 2. Others tumours than carcinoids — differentiated NET tumours (gastrinoma, islet cell, MCT; pheochromocytoma, paraganglioma)

Patient	Age	Histology	Localisation	Clinical details
27	64	Pheochromocytoma	Adrenal	Right adrenal intra-abdominal mass
28	72	Pheochromocytoma	Adrenal	Left adrenal tumour
29	31	Gastrinoma	Left lobe liver	Recurrent gastrinoma — 1975
30	54	Gastrinoma	Liver	Aggressive liver gastrinoma
31	35	Gastrinoma	Tail of pancreas	Metastatic gastrinoma; MEN I
32	45	Gastrinoma	Pancreas	Liver metastasis
33	72	Islet-cell	Pancreas	Islet-cell tumour
34	47	Paraganglioma	Stomach	Stomach paraganglioma
35	40	Paraganglioma	Lung peripheral	Recurrent secreting paraganglioma
36	48	MCT	Thyroid	MCT & neck lymph node involvement

Table 3. NET indeterminate and others with lesions with NET signs

Patient	Age	Histology	Localisation	Clinical details
37	61	NET	Abdomen	Undifferentiated NET, liver metastasis
38	74	NET	Pancreas head	Undifferentiated NET tumour
39	49	NET	Ampulla	Recurrent NET undifferentiated 1996
40	42	NET	Head of pancreas	Recurrent undifferentiated NET
41	48	NET	Pancreas	Pancreatic tumour with liver metastasis
42	52	NET	Pancreas	Pancreatic tumour with liver metastasis
43	70	NET	No origin	Liver metastasis
44	57	NET	Head of pancreas	Pancreatic NET
45	49	HCC/NET atypical	Liver, adrenals	Liver secondaries
46	57	NET/HCC atypical	Pancreas/liver	NET or atypical HCC of the liver
47	73	Solitary fibrous tumour	Retroperitoneal tumour	Large retroperitoneal mass
48	65	Fibrolamellar HCC	Liver	Recurrent fibrolamellar tumour of the liver

MEN I — Multiple endocrine neoplasia type I, NET — neuroendocrine tumour, HCC — Heparocellular carcinoma, Mts — metastases, MCT — Medullary Carcinoma of Thyroid

In 22 patients ^{111}In Octreotide was the most effective modality (e.g. Fig. 3). One patient had no preference with any imaging approach.

As not all patients had subsequent ^{123}I mIBG study, comparison was performed only for CT and ^{111}In Octreotide studies. Results indicated that octreotide was more effective than CT in detection of the number of organs involved by cancer (Wilcoxon Matched Pairs test $p < 0.001$) and also overall number of lesions detected using CT and ^{111}In Octreotide was larger than CT alone (Wilcoxon Matched Pairs test $p < 0.01$). The number of liver deposits indicates that ^{111}In Octreotide was more efficacious than CT (Wilcoxon Matched Pairs test $p < 0.05$).

Additional analysis was performed in selected population of patients with carcinoid tumours, those with other types of NET tumours (including: islet cell carcinoma, malignant paraganglioma, gastrinoma, MCT, pheochromocytoma). The last group consists of undifferentiated NET tumours and also other tumour types expressing somatostatin receptors (2 hepatocellular carcinoma; single HCC fibrolamellar type and single fibrous tumour). Cross-sectional analysis showed no significant difference between CT and the scintigraphic techniques independent of the type of the cancers (Mann-Whitney U test, $p > 0.05$).

Discussion

The diagnostic approach in disseminated neuroendocrine tumours (NET) remains a significant clinical problem. In patients with (symptomatic) carcinoid, in one study involving 154 consecutive patients with gastrointestinal carcinoid tumours, 60% of those found at surgery were asymptomatic and only 40% were symptomatic [15]. This type of tumours is a clinical challenge because the time from the onset of symptoms until the diagnosis is frequently delayed, varying from 1 to 2 years in different studies [16].

Currently a number of techniques including gastrointestinal endoscopy, gastrointestinal barium radiographs, chest radiographs, ultrasound, computed tomography (CT), magnetic resonance imaging (MRI), angiography, endoscopic ultrasound, selective venous sampling for various hormones, and various forms of radionuclide scanning (radiolabelled somatostatin receptor scintigraphy (Octreotide), iodinated metaiodobenzylguanidine (mIBG)) have all been used to determine the location of the primary tumour as well as the tumour extent [9, 17–21].

Bronchial carcinoids are usually detected by chest radiography, CT or occasionally by bronchoscopy [18]. In our study only 2 patients presented with lung NETs, one with bronchial carcinoid

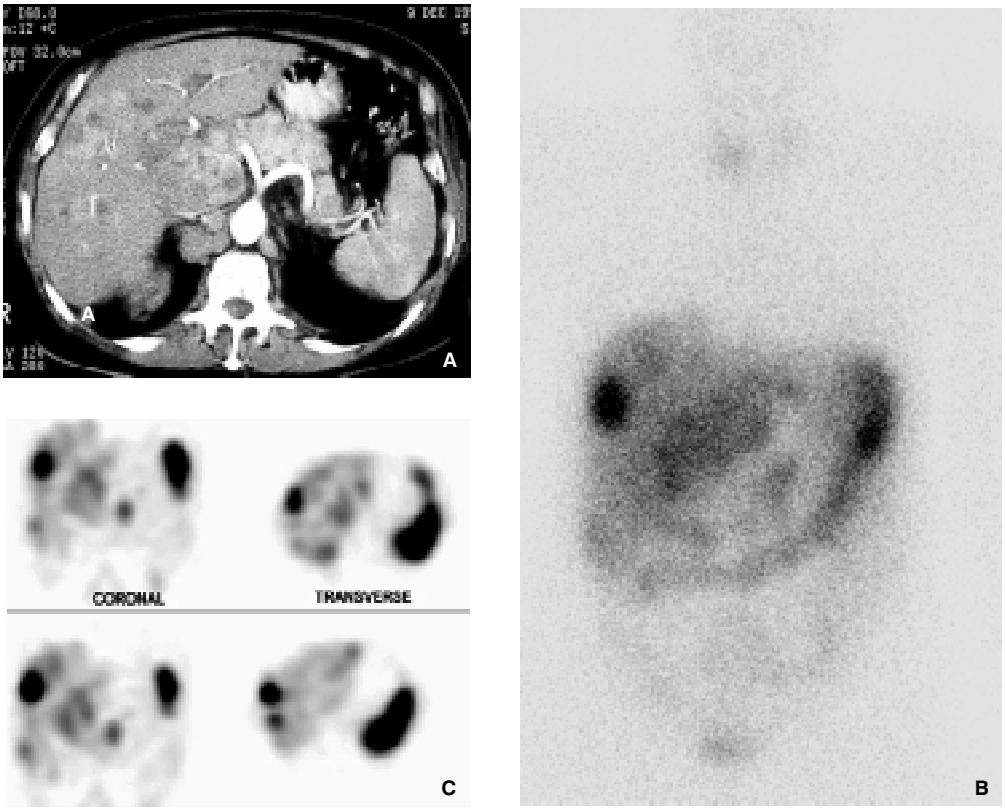

Figure 1. Metastatic carcinoid tumour, at 61-year-old man with primary pancreas head carcinoid. **A.** Triple phase CT with contrast enhancement (10 mm section) shows pancreatic mass, liver metastases and numerous lymph nodes around the IVC and aorta. **B.** and **C.** Whole body and SPECT (coronal and transverse slices) show multiple sites of abnormal uptake within head of pancreas the liver and para-aortic lymph nodes.

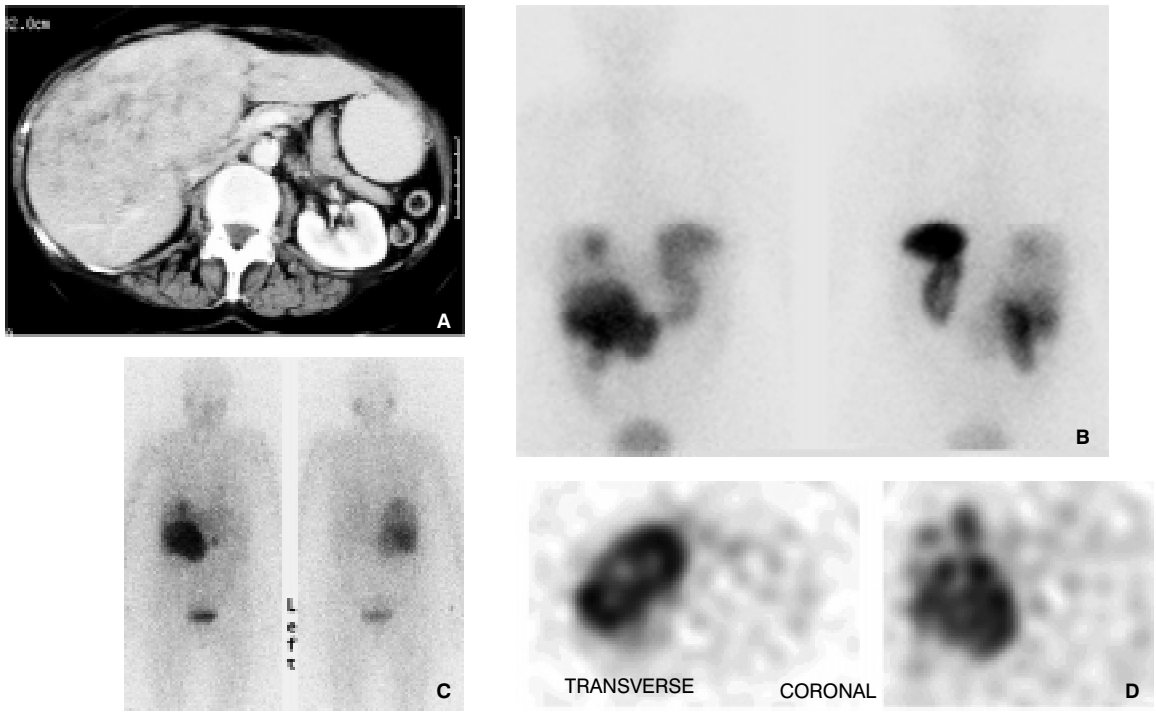

Figure 2. Metastatic carcinoid tumour, at 70-year-old man with primary carcinoid of the caecum, currently with liver deposits. **A.** Triple phase CT with contrast enhancement (10 mm section) shows extensive mass extending from the inferior aspect of segment VIII down into segments V and VI completely replaced and 2 smaller deposits in segment VIII. This huge mass enhances to the same degree as liver parenchyma apart from central areas of presumable necrosis. **B.** Whole Body (WB) In-111 Octrotide scan shows the same distribution of tracer within huge right lobe mass and additional 2 small in segment VIII. **C.** and **D.** WB and SPECT (transverse and coronal) I-123 mIBG images show similar pattern of distribution of radiotracer, additional SPECT shows central part of the tumour with low uptake indicated central part necrosis.

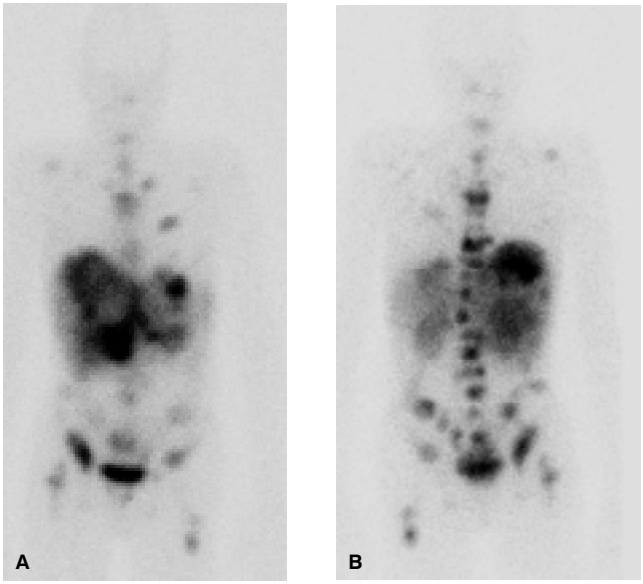

Figure 3. Disseminated carcinoid at 53-year-old man. **A.** and **B.** AP and PA images show widespread areas of increased tracer uptake involving multiple vertebrae, multiple areas in the pelvis, the long bones, the sternum, lesions in the liver and soft tissue in the abdomen.

and another one with lung paraganglioma, both seen in ^{111}In Octreotide study. Extent of the disease, which in lung paraganglioma were also spine and skull, were correctly identified using octreotide study. Bronchial carcinoid was evaluated with addition of single liver deposit also using radionuclide imaging. The bronchial carcinoid tumours are slow growing and often induce airway compression with resultant atelectasis [22]. The primary site of tumour growth or recurrence is precisely localised using standard anatomical approach, as shown in our study, but extent of disease was clearly better assessed using ^{111}In octreotide, which showed additional liver deposit.

Rectal, colonic and gastric carcinoids are almost always detected by gastrointestinal endoscopy, with barium radiographs being generally negative [15, 23–25]. Currently ileal, caecal and right colon tumours are often diagnosed on radiographic studies [17, 26]. The main problem is localising small bowel carcinoids, which may be very small and frequently missed by imaging studies [27]. However our study, like previous reports, confirms high accuracy of radionuclide imaging in tumour detection, also in evaluation of disease extent in this area [7–9].

In our series 14 carcinoid tumours, single paraganglioma and single undifferentiated NET tumour, which primary involved bowel, stomach or duodenum ampulla ^{111}In octretotide and ^{123}I mIBG, were the best modalities in 9 subjects. CT was superior only in 3 cases in tumour detection and evaluation of disease extent. Three other subjects had CT result as good as octreotide study. It should be mentioned that some of these tumours can be localised by angiography, CT scanning or functional imaging but others can be missed with these modalities [21, 27]. Recent studies indicated that CT scanning was generally poor at detection of the primary tumour: ranged from 2% in one study to 17% in the other [21, 27].

Liver deposits are usually well seen on CT scanning. However, previous reports as well as this study support the idea that functional imaging, especially when SPECT technique is performed, is also highly sensitive in assessing number of liver deposits [19–21, 27]. Abdominal carcinoid, whose origin is often appendix, rectum or ileum, first metastasises to abdominal lymph nodes and then to liver. Carcinoid tumours possess high-affinity receptors for somatostatin in 88% of cases, and the somatostatin receptors are present in both the primary tumour and metastases [2, 3, 6, 9].

From 65% to 90% of gastrinomas found at surgery occur in the pancreatic duodenal area [28]. In our group 2 gastrinomas were found within liver (recurrent and aggressive primary tumour). These preoperative imaging studies can identify patients with metastatic spread to the liver. Two other patients had tumours located within pancreas. As previous reports indicated, gastrinomas are frequently multiple and extrapancreatic and additionally in 50% of patients no tumour is found at surgery. Therefore, careful imaging studies can assist the surgeon in localising the tumour [28, 29]. Other modalities like endoscopic ultrasound (EUS) seem to be very sensitive in detection of tumour within pancreas [30].

Conclusion

Because of its sensitivity and ability to image all body areas ^{111}In octreotide should be the initial imaging procedure to localise and establish the extent of the neuroendocrine tumour [19, 20]. Due to nature of NETs any methods which visualised tumour deposits are helpful, including anatomical and function imaging.

Our results confirm the recommendation of the European NET group that functional imaging should be performed in patients with suspected NET.

References

1. Kloppel G, Heitz PU. Classification of normal and neoplastic neuroendocrine cells. Ann NY Acad Sci 1994; 733: 19–23.
2. Langley K. The neuroendocrine concept today. Ann NY Acad Sci 1994; 733: 1–17.
3. Creutzfeldt W. Historical background and natural history of carcinoids. Digestion 1994; 55: 3–10.
4. Jensen RT, Norton JA. Endocrine tumours of the pancreas. In: Yamada T, Alpers BH, Owyang C, et al. eds: Textbook of gastroenterology. Philadelphia: JB Lippincott, 1995: 2131–2162.
5. Kleppel G, Schroder S, Heitz PU. Histopathology and immunopathology of pancreatic endocrine tumours. In: Mignon M, Jensen RT. (eds.). Endocrine tumours of the pancreas: recent advances in research and management. Basel, Switzerland: S Karger, 1995: 120–156.
6. Reubi JC, Laissue,J, Krenning E, Lamberts SWJ. Somatostatin receptors in human cancer: Incidence, characteristics, functional correlates and clinical implications. J Steroid Biochem. Mol Biol 1992, 43, 27–35.
7. Krenning EP, Bakker EP, Breenman WAP, et al. Localisation of endocrine related tumours with radioiodinated analogue of somatostatin. Lancet 1989: 242–244.
8. Jamar F, Fiasse R, Leners N, Pauwels S. Somatastatin imaging with indium-111 pentetreotide in gastr0enteropancreatic neuroendocrine tumours: safety, efficacy and impact on patient management. J Nucl Med 1995: 36: 542–549.
9. Krenning EP, Kwekkeboom DJ, Bakker WH, et al. Somatostatin receptor scintigraphy with [^{111}In-DTPA-*D*-Phe^1] and [^{123}I-Tyr^3]-octreotide: The Rotterdam experience of more than 1000 patients. Eur J Nucl Med 1993: 20: 716–731.

10. Janson ET, Westlin JE, Erikson B, Ahlstrom H. Nilsson S, Oberg K. [^{111}In-DTPA-*D*-Phe^{1}] octreotide scintigraphy in patients with carcinoid tumours: The predictive value for somatostatin analogue treatment. Eur J Endocriol 1994: 131: 577–581.
11. Bravo EL. Evolving concepts in the pathophysiology, diagnosis and treatment of pheochromocytoma. Endocr Rev 1994; 15: 356–368.
12. Werbel SS, Ober KP. Pheochromocytoma: update on diagnosis, localization, and management. Med Clin North Am 1995; 79: 131–153.
13. Francis IR, Glazer GM, Shapiro B, Sisson JC, Gross BH. Complementary roles of CT and ^{131}I-MIBG scintigraphy in diagnosing pheochromocytoma. AJR 1983; 141: 719–725.
14. Hoefnagel CA. Metaiodobenzylguanadine and somatostatin in oncology: role in management of neural crest tumours. Eur J Nucl Med 1994: 21: 561–581.
15. Thompson GB, van Heerden JA, Martin JK, et al. Carcinoid tumours of the gastrointestinal tract: presentation, management and prognosis. Surgery 1985; 98: 1054–1063.
16. Norheim I, Oberg K, Theodorsson-Norheim E, et al. Malignant carcinoid tumors. Ann Surg 1987; 206: 115–125.
17. Vinik AI, McLeod MK, Fig LM, Shapiro B, Lloyd RV, Cho K. Clinical features, diagnosis and localization of carcinoid tumors and their management. Gastroenterol Clin North Am 1989; 18: 865–896.
18. Feldman JM. Carcinoid tumors and the carcinoid syndrome. Curr Probl Surg 1989; 26: 835–885.
19. Krenning EP, Kwekkeboom DJ, Oei HY, et al. Somatostatin-receptor scintigraphy in gastroentero-pancreatic tumors. Ann NY Acad Sci 1994; 733: 496–506.
20. Westlin JE, Janson ET, Arnberg H, Ahlstrom H, Oberg K, Nilsson S. Somatostatin receptor scintigraphy of carcinoid tumours using the [**111In-DTPA-D-Phe**1]-octreotide. Acta Oncol 1993; 32: 783–786.
21. Woodard PK Feldman JM, Paine SS, Baker ME. Midgut carcinoid tumors: CT findings and biochemical profiles. J Comput Assist Tomogr 1995; 19: 400–405.
22. Nessi R, Ricci D, Ricci SB, Bosco M, Blanc M. Bronchial carcinoid tumors: radiologic observations in 49 cases. J Thorac Imaging 1991; 6: 47–53.
23. Gough DB, Thompson GB, Crotty TB, et al. Diverse clinical and pathologic features of gastric carcinoid and the relevance of hypergastrinemia. World J Surg 1994; 18: 473–479.
24. Davies MG, O'Dowd GO, McEntree GP, Hennessey TPJ. Primary gastric carcinoid tumors: a view on management. Br J Surg 1990; 77: 1013–1014.
25. Jetmore AB, Ray NE, Gathright JB Jr, McMullen KM, Hicks TC, Timmeke AE. Rectal carcinoids: the most frequent carcinoid tumor. Dis Colon Rectum 1992; 35: 717–725.
26. Jeffree MA, Barter SJ, Hemingway AP, Nolan DJ. Primary carcinoid tumors of the ileum: the radiological appearances. Clin Radiol 1984; 35: 451–455.
27. Sugimoto E, Lorelius LE, Eriksson B, Oberg K. Midgut carcinoid tumours. Acta Radiol 1995; 36: 367–371.
28. Norton JA, Doppman JL, Jensen RT. Curative resection in Zollinger-Ellison syndrome: results of a 10-year prospective study. Ann Surg 1992; 215: 8–18.
29. Norton JA, Sugarbaker PH, Doppman JL, et al. Aggressive resection of metastatic disease in select patients with malignant gastrinoma. Ann Surg 1986; 203: 352–359.
30. Anderson MA, Carpenter S, Thompson NW, Nostrant TT, Elta GH, Scheiman JM Endoscopic ultrasound is highly accurate and directs management in patients with neuroendocrine tumors of the pancreas. Am J Gastroenterol 2000; 95: 2271–2277.